ACTA CHEMICA SCANDINAVICA 21 (1967) 1265–1276

On the Electrical Properties of KNO_3

J. H. FERMOR and A. KJEKSHUS

Kjemisk Institutt A, Universitetet i Oslo, Blindern, Oslo 3, Norway

The electrical resistivities of single crystals of KNO_3 produced by zone melting and grown from aqueous solution have been measured from room temperature to the melting point, using improved equipment. The results are discussed in relation to other properties of the polymorphic modifications of KNO_3, including the onset of rotational disorder of the nitrate group.

Potassium nitrate is, among the monovalent nitrates, of special interest and is perhaps the least understood, partly because its properties are sensitive to the mode of sample preparation.

On heating KNO_3 from room temperature to the melting point (338°C [1]), two stable modifications occur which have been designated as phases II and I by Bridgman.[2] On cooling a sample of the phase I modification in the absence of water, a third form appears in the temperature range 125—105°C (approximately), which has variously been described as metastable [3] and stable.[4] This form, which exhibits ferroelectricity over a part of its existence range,[4,5] is believed to be identical with the stable phase III occurring at higher pressures.[3] Phases I and III have rhombohedral crystal structures [6,7] while phase II is orthorhombic.[8] There are, however, uncertainties associated with the structural arrangement and motion of the nitrate group in the three modifications.

A single crystal which has been heated through the first order transformation between phases II and I at 127.5°C,[9] does not show the intermediate phase III on cooling, unless its temperature has been raised above that of a recrystallization point in the vicinity of 195°C.[4,10] The above information is summarized in Fig. 1.

Previous electrical measurements performed on KNO_3 above room temperature include the following. The temperature dependence of conductivity for single crystal and polycrystalline samples,[11–15] while the conductivities of pure samples and those doped with a divalent substitutional impurity have been investigated at atmospheric and elevated pressures.[13,15,16] Cleaver *et al.*[13] have demonstrated the Wagner effect [17] in doped polycrystalline KNO_3 (phase I) from which it may be deduced that K^+ vacancies are the dominant charge carriers. In addition, the kinetics of transformation between the phases

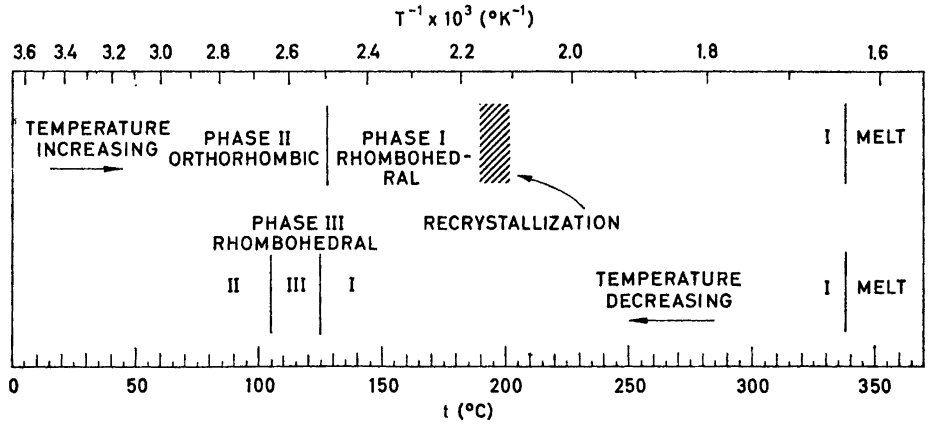

Fig. 1. The polymorphic modifications of KNO_3 above room temperature.

II → I, I → III, and III → II have been investigated by means of the resulting changes in resistivity.[18]

In attempting to use the results of earlier work to obtain an understanding of the electrical conduction process and its dependence on other properties of pure samples, it became apparent that the available data was deficient in the following respects:

(1) There were no results for a phase I single crystal.

(2) No measurements had been performed on zone refined samples of high purity.

(3) The methods of electrical measurement which had been applied were not of the highest accuracy.

In order to overcome these deficiencies, a programme of sample growth and measurement was undertaken in which a variety of a.c. and d.c. methods were applied to zone refined samples and those grown from aqueous solution.

EXPERIMENTAL

(a) *Materials.* All samples were grown using E. Merck AG *p.a.* grade KNO_3 as starting material. The maximum impurity concentrations of the starting material, of samples grown from aqueous solution, and those formed by zone melting are shown in Table 1. The results comprise values supplied by the manufacturer, and those obtained by means of spectrographic, neutron activation, and flame photometric analyses.

Guinier photographs were taken of the sample materials with KCl (Analar, The British Drug Houses Ltd., a = 6.2919 Å [19]) added as an internal standard, using monochromatized Cu$K\alpha_1$-radiation (λ = 1.54050 Å). The deduced unit cell dimensions and volumes are reported in Table 2, which also includes values taken from recent literature. Some variation in lattice parameters is seen; however, all the values of V are in agreement within the error limits stated.

(b) *Single crystal specimens grown from aqueous solution.* Prismatic crystals of a regular hexagonal cross-section were grown from aqueous solution of the starting material. Samples were cleaved from the crystals and ground to a rectangular shape. Samples Nos. 1 and 2 were obtained from the first and third recrystallizations, respectively.

Table 1. Maximum impurity contents of materials used (in ppm).

Impurity	Material			
	Starting (Manufacturers data)	Starting	Crystal from aqueous sol'n	Zone refined crystal
Li		0.01	0.01	0.01
Na	200	100	40	40
Mg		0.1	0.5	0.3
Cl	10			
Ca	10	1	5	3
Fe	3			
Rb		25	1	10
Sr		0.05	0.05	0.05
Cs		0.1	0.1	0.1
Ba		0.5	0.5	0.5
Heavy metals *e.g.* Pb	5			
NH_4	10			
PO_4	5			
SO_4	30			
Water insoluble	50			

Table 2. Unit cell dimensions and volumes determined from Guinier photographs. The limits of error are equal to twice the standard deviation.

Material	a (Å)	b (Å)	c (Å)	V (Å^3)
Merck KNO_3 Starting material	5.4147 ± 0.0008	9.1649 ± 0.0014	6.4268 ± 0.0010	318.90 ± 0.15
Sample from aqueous sol'n	5.4167 ± 0.0014	9.1617 ± 0.0024	6.4311 ± 0.0014	319.16 ± 0.24
Zone refined sample	5.4140 ± 0.0009	9.1642 ± 0.0018	6.4275 ± 0.0012	318.90 ± 0.19
(Swanson *et al.*[20])	5.414	9.164	6.431	319.1

(c) *Preparation of single crystals by zone melting.* The zone refiner used to produce samples Nos. 3, 4, and 5 is shown diagrammatically in Fig. 2. This apparatus provides cylindrical single crystal bars of up to 15 mm diameter and 200 mm length, within quartz tubes which are closed at each end and provided with apertures for filling and the insertion of possible electrodes. Thermocouple and test leads, insulated with alumina, are inserted through closures to the inner tube of the refiner. D.c. is used for both heating elements in order to avoid the injection of spurious signals into the measuring circuits.

The starting material was finely ground in an agate mortar before being transferred to the sample tube which was maintained at a temperature slightly below the melting

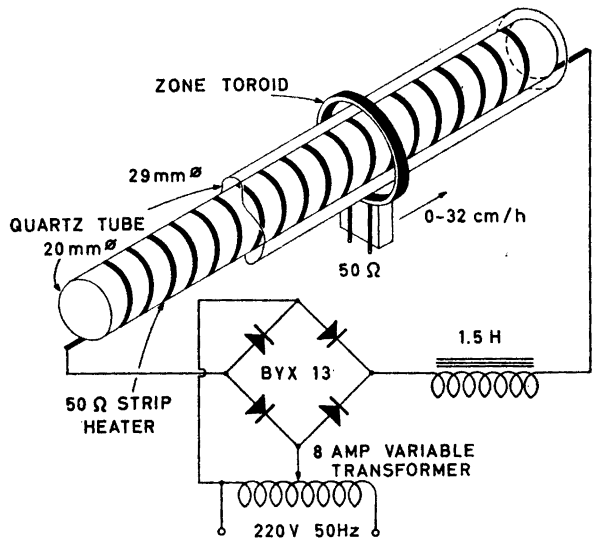

Fig. 2. Zone refiner used in the production and electrical measurement of single crystals of KNO_3 in the phases I and III.

point for a period of 8 h in order to dry the salt. After melting the sample, the temperature was reduced to 300°C and the zone heater set into operation so that a zone of ~ 5 mm width was obtained at a speed of 10 cm/h.

Breakage of the sample tube frequently occurred owing to adhesion between the sample and its container, and a progressive increase in the pressure exerted by the sample with the number of zone passes. This problem was overcome by only partly filling the sample tube, and transferring the purified material to a new tube after a few of the total number of passes (10–20).

Sample No. 3 was cooled over a period of 8 h and removed from the sample tube by crushing the latter in a vice. The mechanical strength of the phase II sample was sufficient to permit the shaping of a specimen.

Where a phase I single crystal was to be investigated, electrodes of spiralled silver wire (ø = 0.2 mm) were introduced into the sample tube together with the starting material.

(d) *Resistance determination by four-terminal method.* In the cases of samples Nos. 1, 2, and 3, the electrical resistance was determined as a function of temperature by the use of equipment which has been described previously.[21,22] The electrical method of measurement consists of a potentiometer bridge in which null electrometers are employed as potential sensing elements. The four-terminal method of connection to the sample has the important advantage that polarization potentials at the current electrodes are excluded from the measured potential. The sample temperature is controlled automatically and measured by means of a platinum thermometer used in conjunction with an improved Mueller bridge circuit.

In applying this and the following methods, the temperature of the sample was held constant for a period of 30 min prior to each observation, except in the case of sample No. 4 where 15 min were allowed.

(e) *Resistance determination by two-terminal d.c. method.* The circuit diagram of the apparatus, which incorporates the prototype instrument of a new kind of electrometer,[23] is shown in Fig. 3. In obtaining a measurement, the electrometer, of resolution 1 mV, is brought to null by adjustment of the calibrated potentiometer E. The value of R is preferably selected such that V lies in the range $2\ E - 11\ E$. The sample voltage and current are calculated from the values of V, R, and E ($> 1\ V$) to within 0.5 and 1.5 %,

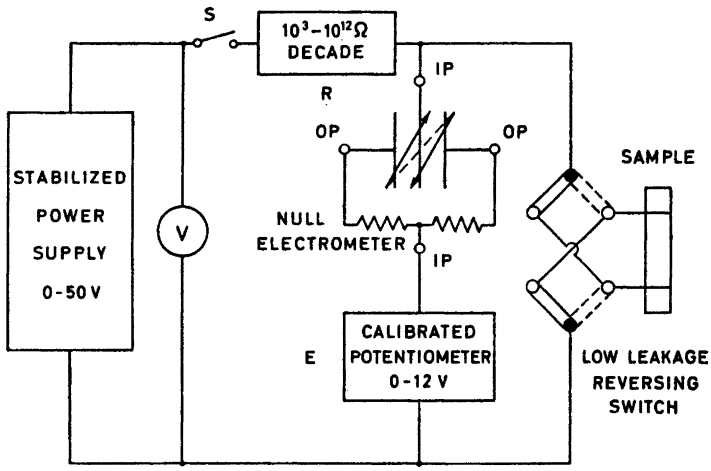

Fig. 3. Circuit diagram for d.c. two-terminal method of resistance measurement.

respectively. With the switch S in the open position, e.m.f.'s from the sample (*e.g.* polarization potentials) may be measured and allowed for in calculating resistance values.

(f) *Resistance determination by two-terminal a.c. method.* Because of the disadvantages inherent in the two-terminal method of connection, an a.c. method of resistance measurement was also developed for use on samples within the zone refiner. A low frequency of operation was chosen as being most likely to provide results consistent with those of the d.c. determination.

As shown in the circuit diagram of Fig. 4, a calibrated voltage source is alternated in resonance with a moving coil galvanometer by means of a motor-driven chopper. In obtaining a measurement, the applied voltage is adjusted to produce a certain amplitude of oscillation in the galvanometer. Initially, a d.c. amplifier was used in conjunction with the galvanometer, but as the extra sensitivity was found to be unnecessary, it was later dispensed with. The series capacitor prevents any asymmetry in the chopper waveform from producing a d.c. component of specimen current. The circuit is calibrated by means of the substitution of standard resistors in place of the sample.

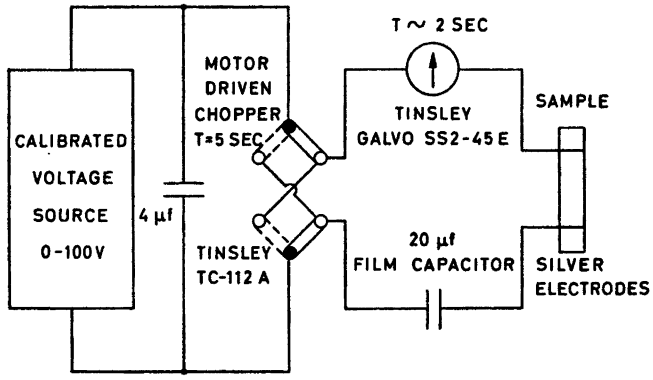

Fig. 4. Circuit diagram for a.c. two-terminal method of resistance measurement.

(g) *Determination of sample geometry.* The separations of electrical contacts on the samples were determined using a travelling microscope (Swift L 201). The dimensions of samples were obtained with the travelling microscope, vernier calipers, and in some cases by weighing the sample of measured length.

RESULTS

(i) *Samples Nos. 1 and 2.* Resistivity along [001] (of the phase II single crystal) is shown as a function of the inverse absolute temperature in Fig. 5 for samples Nos. 1 and 2. The results were obtained using the method of section (d).

The temperature of transition between the phases II and I (the line *BC* of Fig. 5) was approached slowly and the sample resistance fell at the constant temperature $t_{tr} = 128.5 \pm 1.5°C$.

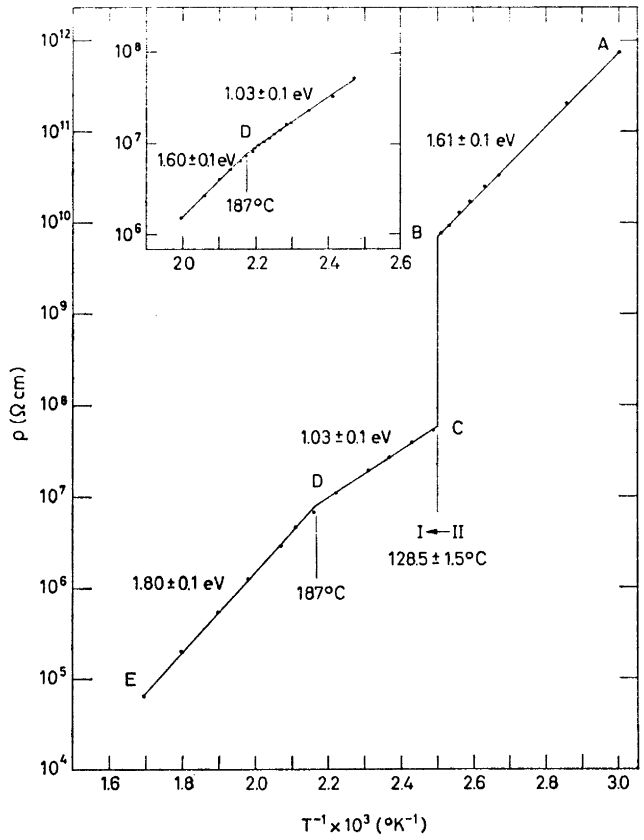

Fig. 5. D. c. resistivity along [001] (in the phase II) as a function of the inverse absolute temperature for sample No. 1. Results for sample No. 2 are shown in the inset figure.

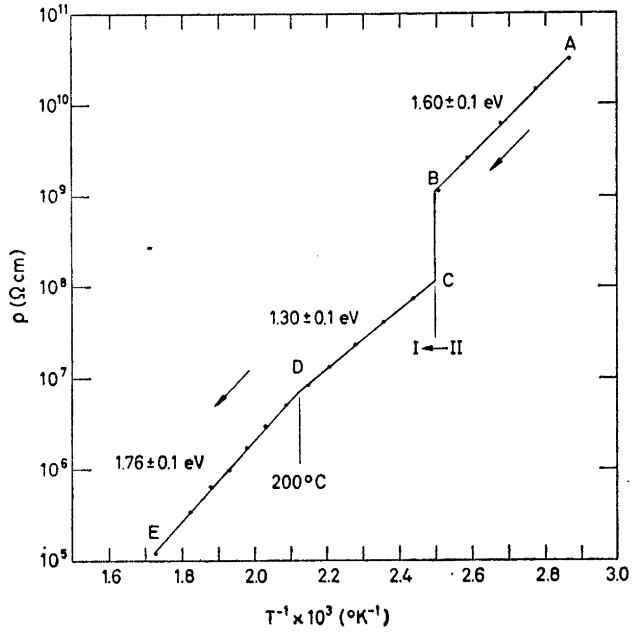

Fig. 6. D. c. resistivity *versus* inverse absolute temperature for sample No. 3.

(ii) *Sample No. 3.* Resistivity along [001] (of the phase I zone refined single crystal) determined as a function of temperature using the method (d) is plotted *versus* the inverse absolute temperature in Fig. 6.

(iii) *Sample No. 4.* Resistivity along [001] (of the phase I zone refined single crystal) determined using the methods of sections (e) and (f) is shown as a function of the inverse absolute temperature in Fig. 7. The d.c. method of section (e) was applied under conditions of decreasing temperature, the measurements being extended beyond the phase I → III transition at ~125°C. On passing through this transition, the sample remained transparent but developed fine cracks at ~1 mm spacings. After returning the sample through the transition to the phase I, the a.c. method of section (f) was applied with increasing temperature to within a few degrees of the melting point.

This comparison was performed in order to investigate the feasibility of collecting data for samples situated within the zone refiner. Both methods of measurement proved to be effective, good agreement being obtained between the two sets of results. The slight deviation seen between the two curves is due to the introduction of fine cracks in the crystal at the phase I → III transition.

(iv) *Sample No. 5.* The a.c. method of section (f) was applied in measuring the temperature dependence of the resistance with decreasing temperature from the melting point. The values of sample resistivity in the phases I and III are shown as a function of the inverse absolute temperature in Fig. 8.

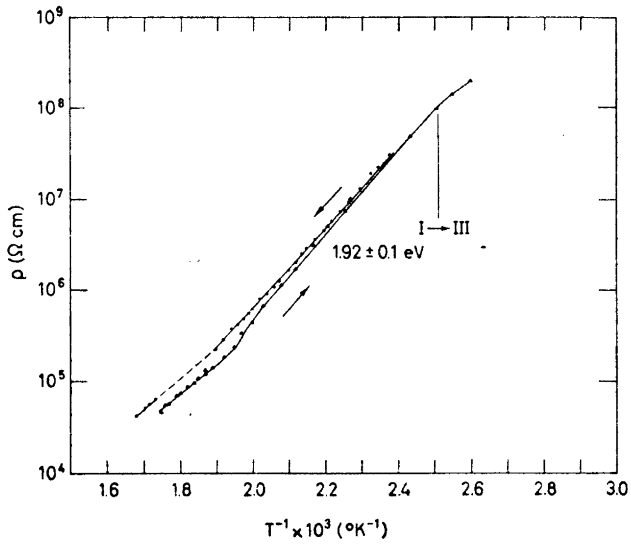

Fig. 7. D. c. resistivity (▲) and a.c. resistivity (●) along [001] as functions of the inverse absolute temperature for sample No. 4.

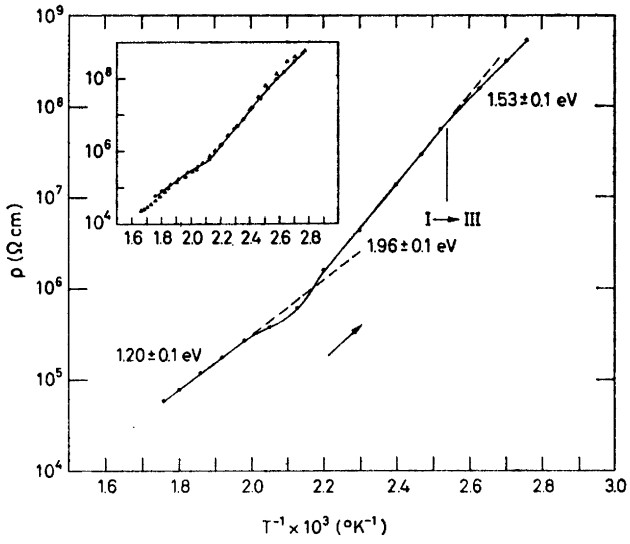

Fig. 8. A. c. resistivity along [001] for phases I and III *versus* the inverse absolute temperature for sample No. 5. Results obtained under decreasing (●) and increasing (▲) temperature are shown in the inset diagram.

As in the case of sample No. 4, cracks were seen to develop at the phase I → III transition.

On increasing the sample temperature, a further set of data was obtained using the same method of measurement. These results, together with the first set of data, are plotted as an inset to Fig. 8.

DISCUSSION

The results shown in the Figs. 5—8 display several interesting and unexpected features and permit a number of tentative deductions concerning the electrical conduction process in KNO_3.

The resistivity of a single crystal grown from aqueous solution shows an essentially linear form AB in the phase II (Fig. 5) which is interrupted by a discontinuity of approximately two orders of magnitude on passing through the phase II → I transition. A change of the same magnitude has been reported by Asao *et al.*,[14] who were unable to record the isothermal nature of the transition since their sample temperature was varied continuously. The corresponding results for a mosaic form phase II crystal, formed by zone refinement show an identical energy parameter $\varepsilon = 1.6 \pm 0.1$ eV at lower resistivity levels in the phase II, and a discontinuity of reduced value at the phase II →I transition. These results lead one to suppose that the type of charge carrier and conduction mechanism is the same in mosaic and single crystals in the phase II and that the discontinuity is the result of the introduction of innumerable crevice-like paths of comparatively low resistance throughout the crystal.

All mosaic crystals (samples Nos. 1, 2, and 3, Figs. 5 and 6) have a characteristic which departs from linearity in the phase I region. At first sight, the results for samples Nos. 1 and 2 appear to lie on two straight lines intersecting at the point D, as shown in Fig. 5. An alternative analytical representation of these results is, however, as follows.

On the basis of an elementary model (see *e.g.* Ioffe [24]), the resistivity of an ionic conductor may be expressed in the form

$$\varrho = \varrho_0 \exp(\varepsilon/2kT) \tag{1}$$

where the parameter ε is given in terms of the carrier activation energy ε_A and translational barrier energy ε_B by

$$\varepsilon = \varepsilon_A + 2\varepsilon_B \tag{2}$$

When two independent conduction mechanisms are active over a given temperature range, each being dominant at an extreme temperature, the conductivity σ may be written for the whole region as

$$\sigma_{\text{total}} = \sigma_1 \exp(-\varepsilon_1/2kT) + \sigma_2 \exp(-\varepsilon_2/2kT) \tag{3}$$

where the values of the parameters ε_1, ε_2, σ_1, and σ_2 may be obtained from the values of the slopes and intercepts of linear portions of the curve remote from the change in slope.

The ε values shown in Fig. 5 are those calculated from the slopes of the lines concerned. Owing to the fact that the lengths of the lines available for measurement between the phase II → I transition and the melting point are rather short, the substitution of these ε values together with the corresponding values of σ in eqn. 3, provides a calculated curve which is a rather poor approxi-

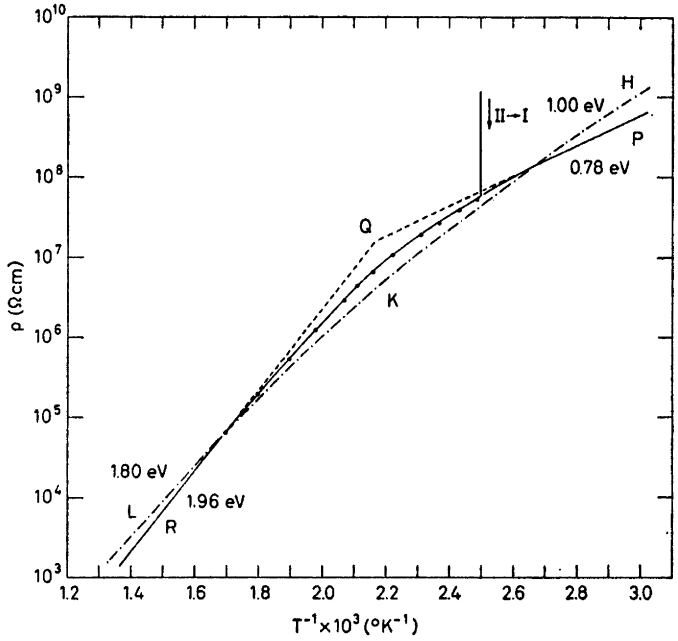

Fig. 9. Experimental results for sample No. 1 in the phase I together with theoretical curves calculated from eqn. 3 using apparent (dotted line) and corrected (unbroken line) values of ε_1, σ_1, ε_2, and σ_2.

mation to the experimental results. This is demonstrated in Fig. 9, where the experimental results for the phase I region have been replotted. It is seen that the curve *HKL* which was calculated as described above, departs significantly from the experimental results. Good agreement between the theoretical curve *PR* and the experimental results has been obtained, however, by means of a process of successive approximation in deriving values of ε_1, σ_1, ε_2, and σ_2. The energy gaps thus obtained ($\varepsilon_1 = 0.78 \pm 0.1$ eV, $\varepsilon_2 = 1.96 \pm 0.1$ eV) differ appreciably from the values apparent from Fig. 5 ($\varepsilon_1 = 1.00 \pm 0.1$ eV, $\varepsilon_2 = 1.80 \pm 0.1$ eV). The broken lines, intersecting at the point *Q*, which has a resistivity value equal to twice that at the point *D* in Fig. 5, are extrapolated from the remote portions of the calculated curve.

In the case of the results shown in Fig. 6 for a zone refined mosaic crystal, the same process of successive approximation leads to the values $\varepsilon_1 = 0.99 \pm 0.1$ eV and $\varepsilon_2 = 2.07 \pm 0.1$ eV which are significantly different from the values derived directly from the lines ($\varepsilon_1 = 1.30 \pm 0.1$ eV and $\varepsilon_2 = 1.76 \pm 0.1$ eV) drawn in Fig. 6.

The forms of the curves shown in Figs. 5 and 6 suggest an interpretation in which the parts *CD* and *DE* of the curves represent extrinsic (impurity) and intrinsic conduction properties, respectively. This possibility may be excluded, however, since the single crystal samples show no transition of this form.

It seems that the departure from linearity of the resistivity of the phase I mosaic crystal may be correlated with certain temperature dependent effects in the sample. Borchert [10] has observed recrystallization phenomena in mosaic samples at about 195°C. This recrystallization is necessary if the sample is to transform into the phase III on cooling.[4] Calorimetric results for phase I KNO_3 [25,26] show that the first order phase II → I transformation is followed at higher temperatures by an exponentially shaped return to the extrapolated C_p curve. This may be interpreted as a completing of the order-disorder process associated with this transition,[27] probably an orientational disorder of the nitrate group. The parts *CD* of the curves for mosaic samples (Figs. 5 and 6) therefore refer to a transitional interval for an inhomogeneous sample and the energy parameter should not be interpreted in terms of the simple model, which is, however, assumed to apply at higher temperatures. This region may reflect the closing off of the crevice-like conduction paths, *e.g.* as a result of the disordering of the nitrate groups situated on the surface of the crystallites.

The results for single crystal samples in the phases I and III differ greatly from those of the mosaic specimens. The more precise results (Fig. 8) show three distinct linear sections. The part *AB* applies to the phase III and shows supercooling into what is normally the phase II temperature range. In the phase I region, the curve shows a decrease of energy gap with increasing temperature as compared with an increase in the case of mosaic samples. The form of the curve may result from pressure exerted on the sample by its container. This explanation appears unlikely, however, in view of the high pressures which would be necessary in order to produce the observed deviation from linearity.[17] Alternatively, the explanation may lie in the effect on the energy parameters of a progressive increase in the proportion of disordered nitrate groups in the temperature range 128.5—190°C (approximately). A disordered nitrate group may be expected to produce periodic fluctuations in potential at neighbouring lattice and interstitial sites.

CONCLUSION

The electrical conductivity of KNO_3 is highly dependent on whether the sample is a single crystal or of mosaic form. In the latter case conduction is predominantly along crevices between the grains. In the phase II, both single crystal and mosaic samples exhibit an energy parameter $\varepsilon = 1.6 \pm 0.1$ eV, while a somewhat lower value is found for the phase III region.

In the phase I, mosaic and single crystals show entirely different forms of temperature dependence of resistivity which is thought to be influenced by disorder of the nitrate group. The results may be represented by two single term exponential expressions valid over restricted regions or a sum of two exponential expressions for the whole region. The interpretation of the wide range of ε values ($1.0 \pm 0.1 - 2.1 \pm 0.1$ eV) determined within the phase I region must await a more detailed understanding of the phenomena involved.

Acknowledgements. This work was made possible by the kind provision of laboratory facilities by Professor H. Haraldsen and the financial support of *Norges almenvitenskapelige forskningsråd.*

REFERENCES

1. Kelley, K. K. *U. S. Bur. Mines, Bull.* **584** (1960).
2. Bridgman, P. W. *Proc. Am. Acad. Arts Sci.* **51** (1916) 579.
3. Kracek, F. C. *J. Phys. Chem.* **34** (1930) 225.
4. Sawada, S., Nomura, S. and Asao, Y. *J. Phys. Soc. Japan* **16** (1961) 2486.
5. Yanagi, T. *J. Phys. Soc. Japan* **20** (1965) 1351.
6. Tahvonen, P. E. *Ann. Acad. Sci. Fennicae, Ser. A I* **1947** No. 44.
7. Barth, T. F. W. *Z. physik. Chem.* **B 43** (1939) 448.
8. Wyckoff, R. W. G. *Crystal Structures, Vol II*, Interscience, New York 1948, Sect. VII.
9. Arell, A. *Ann. Acad. Sci. Fennicae, Ser A VI* **1962** No. 101.
10. Borchert, W. *Z. Krist.* **95** (1936) 28.
11. Foussereau, M. G. *Ann. Chim. Phys.* [6] **5** (1885) 317.
12. Jaffray, J. *Compt. Rend.* **230** (1960) 525.
13. Cleaver, B., Rhodes, E. and Ubbelohde, A. R. *Discussions Faraday Soc.* **32** (1961) 210.
14. Asao, Y., Yoshida, I., Ando, R. and Sawada, S. *J. Phys. Soc. Japan* **17** (1962) 442.
15. Cleaver, B. *Z. physik. Chem. (Frankfurt)* **45** (1965) 346.
16. Cleaver, B. *Z. physik. Chem. (Frankfurt)* **45** (1965) 359.
17. Koch, E. and Wagner, K. *Z. physik. Chem.* **B 38** (1938) 295.
18. Weidenthaler, P. *Collection Czech. Chem. Commun.* **30** (1965) 629.
19. Hambling, P. G. *Acta Cryst.* **6** (1953) 98.
20. Swanson, H. E., Fuyat, R. K. and Ugrinic, G. M. *Natl. Bur. Std. (U.S.) Circ.* **539** III (1954), p. 58.
21. Fermor, J. H. and Kjekshus, A. *Rev. Sci. Instr.* **36** (1965) 763.
22. Fermor, J. H. and Kjekshus, A. *Tidskr. Kjemi, Bergvesen Met.* **27** (1967) 28.
23. Fermor, J. H. and Kjekshus, A. *Rev. Sci. Instr.* **38** (1967). *In press.*
24. Ioffe, A. F. *Physics of Semiconductors*, Infosearch Ltd. London 1960, pp. 2—19.
25. Miekk-Oja, H. *Ann. Acad. Sci. Fennicae, Ser A I* **1941** No. 7.
26. Sokolov, V. A. and Schmidt, N. E. *Izv. Sektora Fiz.-Khim. Analiza, Inst. Obshch. Neorgan. Khim. Akad. Nauk SSSR* **27** (1956) 217.
27. Newns, D. M. and Staveley, L. A. K. *Chem. Rev.* **66** (1966) 267.

Received December 23, 1966.